

# A Comparative CEST NMR Study of Slow Conformational Dynamics of Small GTPases Complexed with GTP and GTP Analogues\*\*

Dong Long, Christopher B. Marshall, Guillaume Bouvignies, Mohammad T. Mazhab-Jafari, Matthew J. Smith, Mitsuhiro Ikura, and Lewis E. Kay\*

The Ras superfamily of small GTPases are important intracellular signaling molecules, the functions of which are determined by the binding of guanosine nucleotides (GTP = guanosine triphosphate and GDP = guanosine diphosphate).<sup>[1]</sup> The GTP-bound (“active”) states of these enzymes are capable of interacting with specific downstream effector proteins, thus eliciting a wide range of cellular responses.<sup>[2,3]</sup> Mutations that reduce the rate of GTP hydrolysis and thus increase the lifetime of the active GTP-bound state are frequently oncogenic and contribute to the development and metastasis of human cancers.<sup>[4]</sup> Elegant <sup>31</sup>P NMR studies of GTP-bound Ras showed that the enzyme interconverts between two states, a minor conformer termed state 1 and a major species designated state 2.<sup>[5–9]</sup> Similar conformational dynamics have been observed in other Ras family GTPases as well.<sup>[10–12]</sup> State 2 is generally regarded as the conformation competent for binding effector proteins, whereas state 1 exhibits significantly reduced affinity for these molecules.<sup>[5–7,13,14]</sup> Stabilization of the low-affinity state 1 was hence suggested as a strategy to inhibit Ras–effector interactions so as to reduce oncogenic signaling.<sup>[15–17]</sup> For example, Zn<sup>2+</sup>–bis(2-picolyl)amine complexes<sup>[18]</sup> were found to stabilize state 1 and inhibit Ras–effector interactions by binding to an allosteric site, albeit with low (millimolar) affinity.

The intrinsic GTPase activity of Ras leads to the conversion of Ras-GTP to Ras-GDP within a few hours at room temperature, imposing a practical limit on the duration of experiments that can be performed with physiological GTP. For this reason, stable GTP analogues, including guanosine 5′-[β,γ-imino]triphosphate (GppNHp), guanosine 5′-O-[γ-thio]triphosphate (GTPγS), and guanosine 5′-[β,γ-methylene]triphosphate (GppCH<sub>2</sub>p) that resist hydrolysis have been used for structural studies of activated GTPases, including characterization of states 1 and 2 of Ras and the kinetics and

thermodynamics of their interconversion.<sup>[5,6,8,14–19]</sup> However, these modifications that stabilize GTP are known to affect the conformational equilibrium between the two states of Ras.<sup>[7–9]</sup> Moreover, the attachment of the mant fluorophore commonly used to probe nucleotide hydrolysis and exchange rates can significantly perturb the kinetics of these processes for several GTPases.<sup>[20]</sup> Therefore, conclusions from studies of small GTPases using GTP analogues must be validated rigorously.

One-dimensional <sup>31</sup>P NMR spectroscopy has been used to explore conformational dynamics in a number of GTPases using the nucleotide as a probe,<sup>[5–9]</sup> focusing in particular on the γ-phosphorous of GTP, which has distinct chemical shifts for states 1 and 2. It is also of interest to address conformational exchange in these systems through direct studies of the proteins as well. O’Connor and Kovrigin used <sup>15</sup>N relaxation dispersion<sup>[21,22]</sup> to characterize the millisecond backbone fluctuations in Ras-GppNHp at room temperature.<sup>[23]</sup> However, as we describe below the same approach cannot be applied to the physiological Ras-GTP complex. Herein, we introduce a general approach for characterizing the equilibrium conformational exchange of small GTPases complexed with GTP using an interleaved chemical exchange saturation transfer (CEST) experiment that effectively suppresses systematic errors in extracted exchange parameters caused by GTP hydrolysis. We demonstrate that CEST spectroscopy<sup>[24,25]</sup> is a powerful method for characterizing slow conformational exchange in the small GTPases Ras and Rheb (Ras homolog enriched in brain). The kinetics and thermodynamics of the interconversion between the major and minor conformational states of these proteins are quantified for GTP-, GTPγS-, and GppNHp-bound forms, showing distinct differences, in particular for the GppNHp analogue of each enzyme.

Because the timescale of intrinsic hydrolysis of GTP by Ras at room temperature<sup>[26,27]</sup> challenges collection of the 2D NMR measurements necessary to probe protein dynamics using multiple sites, we explored the possibility of performing experiments at lower temperature. Quantification of intrinsic GTP hydrolysis by Ras and Rheb using a real-time NMR assay<sup>[28]</sup> revealed that GTP hydrolysis rates can be reduced by an order of magnitude by decreasing the temperature from 25 to 5 °C (Figure 1). The concomitant extension of the lifetimes of the GTP-bound enzymes from hours to days facilitated the collection of <sup>15</sup>N relaxation experiments for characterizing conformational exchange.

The <sup>15</sup>N Carr–Purcell–Meiboom–Gill (CPMG) relaxation dispersion approach<sup>[21,22]</sup> previously used to study conformational exchange in Ras-GppNHp, 25 °C<sup>[23]</sup> is not applicable to Ras-GTP at 5 °C. First, the relative populations of intercon-

[\*] Dr. D. Long, Dr. G. Bouvignies, Prof. L. E. Kay  
 Departments of Molecular Genetics, Biochemistry, and Chemistry  
 University of Toronto, Toronto, Ontario M5S 1A8 (Canada)  
 E-mail: kay@pound.med.utoronto.ca

Dr. C. B. Marshall, M. T. Mazhab-Jafari, Dr. M. J. Smith,  
 Prof. M. Ikura  
 Ontario Cancer Institute, University Health Network  
 Department of Medical Biophysics, University of Toronto (Canada)

[\*\*] D.L. is the recipient of a Canadian Institutes of Health Research (CIHR) postdoctoral fellowship. M.I. and L.E.K. hold Canada Research Chairs in Biochemistry. This work was supported by grants from the CIHR, NSERC, CRS, and CCSRI. GTP = guanosine triphosphate and CEST = chemical exchange saturation transfer.



Supporting information for this article is available on the WWW under <http://dx.doi.org/10.1002/anie.201305434>.

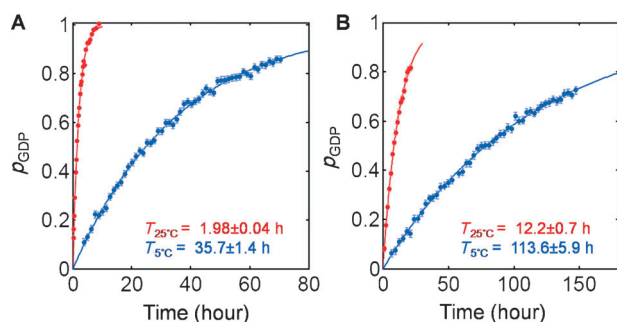


**Figure 1.** Time course of the hydrolysis of GTP in samples of a) Ras-GTP and b) Rheb-GTP at 25 °C (red) and 5 °C (blue). Data for the hydrolysis profile of Ras-GTP, 25 °C, is taken from our previous work<sup>[26]</sup> and shown here for completeness.

verting states 1 and 2 are much more skewed than for the GppNHp complex and second the lower temperature necessary to preserve the GTP-bound complex slows down the conformational exchange process. Both attenuate the contribution of exchange to transverse relaxation, leading to small CPMG dispersion profiles ( $R_{ex} < 4 \text{ s}^{-1}$ ; see the Supporting Information), complicating quantification of exchange parameters. We therefore used a recently developed  $^{15}\text{N}$  CEST experiment<sup>[24]</sup> to probe slow time-scale exchange processes. Here, a series of 2D  $^{15}\text{N}$ - $^1\text{H}$  correlation spectra are recorded with a weak  $^{15}\text{N}$  radio frequency (rf)  $B_1$  field, and the intensities of the major state (“visible”) correlations are quantified as a function of the position of the  $B_1$  field. When the weak rf field is coincident with the resonance frequency of a peak from the major state (“visible” correlation), the peak intensity decreases because of a well-known saturation effect. Similarly, when the  $B_1$  field is applied at the resonance position of the corresponding peak from the minor conformer (“invisible” correlation), the intensity of the peak from the major correlation decreases again, in this case from a transfer of the rf perturbation mediated by the chemical exchange between the states. The result is a series of CEST profiles, ideally one for each (amide) correlation derived from the major state, showing dips in intensity at the chemical shifts of both the major (visible) and minor (invisible) conformers (Figure 2). For residues where the chemical shifts of the major and minor states are degenerate, only a single dip will be observed. By recording the experiment in an interleaved manner whereby the position of the  $B_1$  field is incremented prior to the  $^{15}\text{N}$   $t_1$  evolution delay (indirect detection; see the Supporting Information) the effect of hydrolysis is to accelerate the decay of signal during  $t_1$  with a rate given by Equation (1),

$$R_2^{\text{app}} = R_2 + R_{\text{ex}} + k_{\text{hydro}} \Delta t / DW \quad (1)$$

where  $k_{\text{hydro}}$  is the GTP hydrolysis rate,  $\Delta t$  is the time elapsed between successive  $t_1$  points and  $DW$  is the dwell time in the indirect dimension. The last term in Equation (1) contributes less than  $20 \text{ s}^{-1}$  to  $R_2^{\text{app}}$  in the CEST experiments described below. As the intensities of peaks analyzed in model fitting are normalized with respect to those obtained from a refer-

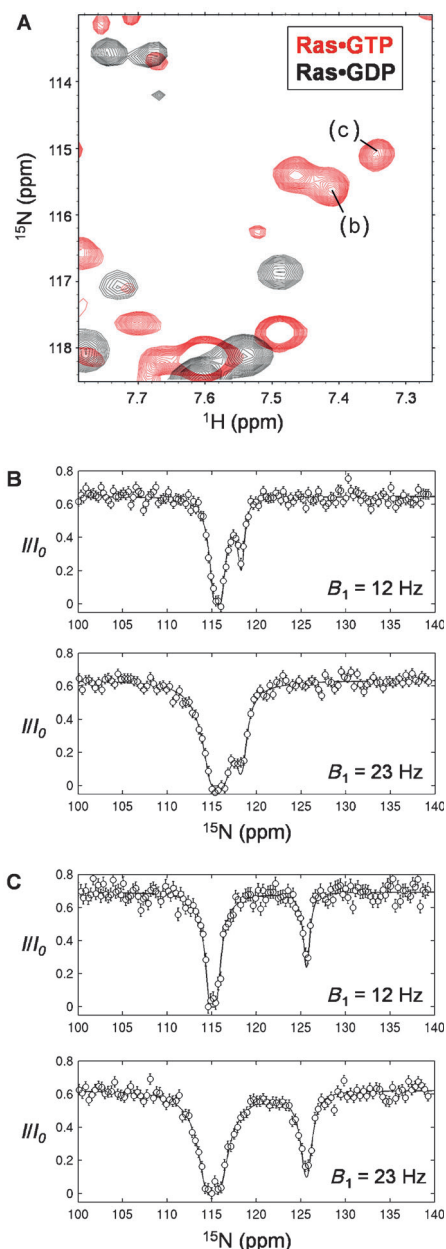


**Figure 2.** Conformational exchange of Ras-GTP probed by  $^{15}\text{N}$  CEST NMR spectroscopy. A) Overlay of 2D  $^{15}\text{N}$ - $^1\text{H}$  correlation spectra of Ras-GTP (red) and Ras-GDP (black), 14.0 T, 5 °C. The intensities of peaks b and c were analyzed to generate the corresponding CEST profiles in panels B and C, respectively. Only correlations from the major state conformer (state 2) are observed in HSQC spectra. B,C) Representative CEST profiles derived from datasets measured using weak  $B_1$  field strengths as indicated for two well-resolved Ras-GTP peaks. Values of  $I$  and  $I_0$  correspond to the intensities of major state cross-peaks recorded with and without the relaxation time,  $T_{\text{ex}}$ , during which the weak  $B_1$  field is applied.<sup>[24]</sup>

ence plane recorded in an interleaved manner at the same time as the rest of the dataset, artifacts associated with GTP hydrolysis are effectively suppressed (subsumed in the relaxation rate). Thus, accurate exchange parameters can be extracted.

CEST profiles of residues from the GTP-bound species, the resonances of which do not overlap those of the GDP-bound protein, were analyzed as described previously (see the Supporting Information). Data sets were recorded at a pair of  $B_1$  fields and profiles of all residues with nondegenerate major/minor state chemical shifts were fit to a model of two-site chemical exchange (Figure 2). Likewise, CEST experiments were recorded on samples of Ras complexed with GppNHp and GTP $\gamma$ S. Previously,  $^{31}\text{P}$  spectra of GTP, GppNHp, and GTP $\gamma$ S complexed with Ras showed that all three Ras forms exist predominantly in state 2, with the population of state 1 significantly higher for Ras-GppNHp.<sup>[8,9]</sup> In this sense GTP $\gamma$ S appears to be a better analogue of physiological GTP than GppNHp, although exchange rates between the states were not reported for Ras-GTP $\gamma$ S.<sup>[8]</sup> Here we use protein CEST spectroscopy to quantify the populations of states 1 and 2 and the exchange rates for their interconversion,  $k_{\text{ex}}$ , for Ras complexed with GTP, GppNHp, and GTP $\gamma$ S (see Table S1 in the Supporting Information). Distributions of  $k_{\text{ex}}$  and  $p_E$ , the population of the minor state (state 1), were obtained using a Monte Carlo simulation<sup>[29]</sup> as described in the Supporting Information (Figure 3 A). Notably, Ras-GTP, Ras-GTP $\gamma$ S and Ras-GppNHp exhibit distinct ( $k_{\text{ex}}, p_E$ ) distributions. The kinetics and thermodynamics of

interconversion of Ras-GTP $\gamma$ S are most similar to Ras-GTP, with nearly identical  $p_E$  values and slightly higher exchange rates (see Table S1). By contrast, Ras-GppNHp exhibits substantially higher  $k_{\text{ex}}$  and  $p_E$  parameters relative to Ras-GTP, indicating that GppNHp does not mimic GTP as well as GTP $\gamma$ S. Interestingly, the  $k_{\text{ex}}$  value we obtain for Ras-GTP ( $72.3 \pm 10.1 \text{ s}^{-1}$ ) at 5°C is an order of magnitude larger than that previously estimated at the same temperature<sup>[9]</sup> using the  $\gamma$ -phosphorous of GTP as a probe ( $7 \pm 2 \text{ s}^{-1}$ ).

To explore the generality of our results we carried out  $^{15}\text{N}$  CEST experiments on the small GTPase Rheb complexed with GTP, GppNHp, and GTP $\gamma$ S (Figure 3 B and Figure S1). Rheb has distinct biological properties and structural features in relation to Ras,<sup>[30]</sup> including a low intrinsic GTP hydrolysis rate (Figure 1) and a nucleotide binding site that is more closed in the GTP-bound state. Thus a comparative dynamics study of Rheb versus Ras is of interest, although to our knowledge the structural dynamics of Rheb have not been characterized previously. As with Ras, the CEST profiles obtained for Rheb clearly showed an exchange between major and minor conformers. In addition, ( $k_{\text{ex}}, p_E$ ) distributions obtained for Rheb in complex with GTP, GTP $\gamma$ S and GppNHp do not overlap, but those for GTP and GTP $\gamma$ S are very similar, whereas the distribution for GppNHp is again distinct, Figure 3. It is clear that for Rheb, GTP $\gamma$ S better mimics the equilibrium interconversion between major and minor states associated with native GTP. Interestingly, in the static crystallographic models of Rheb, no discernable difference was observed between Rheb-GTP and Rheb-GMPPNP.<sup>[30]</sup> Although the structural differences between the interconverting states for Rheb remain to be elucidated in further studies, it may be that the exchange process in this case is between a closed and partially open GTP binding site.

Characterizing the slow conformational dynamics of activated GTPases in relation to function, in particular for Ras, has been the subject of study for many years.<sup>[5,7,18]</sup> Recent efforts have focused on manipulating the conformational equilibrium between states 1 and 2 of activated Ras through the use of small molecules as a promising approach for the development of future anti-cancer drugs.<sup>[16–18]</sup> In this context it is clear that an understanding of the kinetics and thermodynamics of the interconversion between different functional states in these important drug targets is critical. Using a recently developed  $^{15}\text{N}$  CEST NMR approach focusing on backbone amide probes, we have shown that the exchange parameters are similar for GTP $\gamma$ S- and GTP-bound states of both Ras and Rheb, but quite different for the GppNHp nucleotide. Ras-GppNHp has been used as a mimic for identification of interacting small molecules that stabilize state 1 of GTP-bound Ras.<sup>[16–18]</sup> The increased population of state 1 ( $p_E$ ) associated with the GppNHp analogue may lead, however, to overestimation of the effectiveness of selective inhibitors that bind to state 1. Our results emphasize that the affinity and kinetics of GTPase interactions with binding partners should be interpreted with caution when GTP analogues are used. The conformational interconversion described here for Ras and Rheb is likely to be common to other members<sup>[10–12]</sup> of the Ras superfamily and protein CEST spectroscopy is anticipated to be a generally applicable

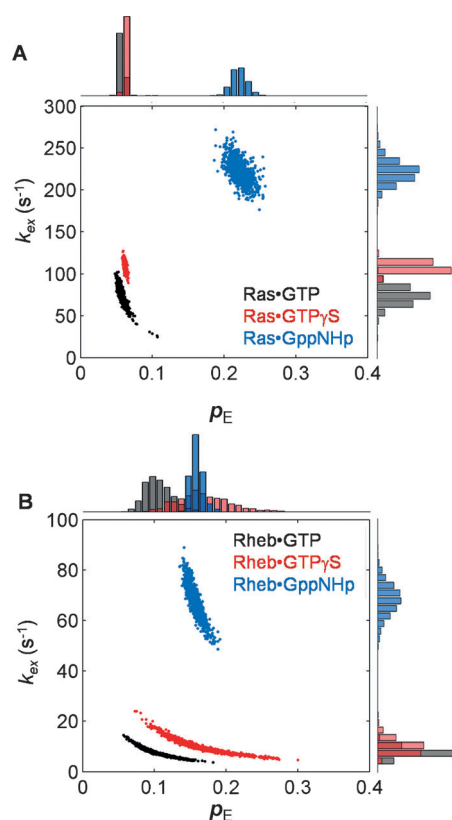


**Figure 3.** Conformational exchange parameters ( $k_{\text{ex}}$  and  $p_E$ ) of A) Ras and B) Rheb complexed with GTP (black), GTP $\gamma$ S (red), and GppNHp (blue) obtained from a global fit of all CEST profiles selected as described in the Supporting Information. Distributions of  $k_{\text{ex}}$  and  $p_E$  were obtained by Monte Carlo analyses,<sup>[29]</sup> (see the Supporting Information). Shown along the x and y axes are histograms of  $p_E$  and  $k_{\text{ex}}$ , respectively.

method for characterizing exchange processes in quantitative detail in these systems as well.

Received: June 24, 2013

Published online: August 22, 2013

**Keywords:** conformational dynamics · enzymes · NMR spectroscopy · protein dynamics · proteins

- 
- [1] K. Wennerberg, K. L. Rossman, C. J. Der, *J. Cell Sci.* **2005**, *118*, 843–846.
- [2] D. S. Goodsell, *Oncologist* **1999**, *4*, 263–264.
- [3] L. J. Saucedo, X. Gao, D. A. Chiarelli, L. Li, D. Pan, B. A. Edgar, *Nat. Cell Biol.* **2003**, *5*, 566–571.
- [4] D. Hanahan, R. A. Weinberg, *Cell* **2000**, *100*, 57–70.
- [5] H. R. Kalbitzer, M. Spoerner, P. Ganser, C. Hozsa, W. Kremer, *J. Am. Chem. Soc.* **2009**, *131*, 16714–16719.
- [6] M. Spoerner, C. Herrmann, I. R. Vetter, H. R. Kalbitzer, A. Wittinghofer, *Proc. Natl. Acad. Sci. USA* **2001**, *98*, 4944–4949.
- [7] M. Geyer, T. Schweins, C. Herrmann, T. Prisner, A. Wittinghofer, H. R. Kalbitzer, *Biochemistry* **1996**, *35*, 10308–10320.
- [8] M. Spoerner, A. Nuehs, C. Herrmann, G. Steiner, H. R. Kalbitzer, *FEBS J.* **2007**, *274*, 1419–1433.
- [9] M. Spoerner, C. Hozsa, J. A. Poetzel, K. Reiss, P. Ganser, M. Geyer, H. R. Kalbitzer, *J. Biol. Chem.* **2010**, *285*, 39768–39778.
- [10] J. Liao, F. Shima, M. Araki, M. Ye, S. Muraoka, T. Sugimoto, M. Kawamura, N. Yamamoto, A. Tamura, T. Kataoka, *Biochem. Biophys. Res. Commun.* **2008**, *369*, 327–332.
- [11] T. Meierhofer, I. C. Rosnizeck, T. Graf, K. Reiss, B. König, H. R. Kalbitzer, M. Spoerner, *J. Am. Chem. Soc.* **2011**, *133*, 2048–2051.
- [12] M. Geyer, R. Assheuer, C. Klebe, J. Kuhlmann, J. Becker, A. Wittinghofer, H. R. Kalbitzer, *Biochemistry* **1999**, *38*, 11250–11260.
- [13] W. Gronwald, F. Huber, P. Grünewald, M. Spörner, S. Wohlge-muth, C. Herrmann, H. R. Kalbitzer, *Structure* **2001**, *9*, 1029–1041.
- [14] M. Araki, F. Shima, Y. Yoshikawa, S. Muraoka, Y. Ijiri, Y. Nagahara, T. Shirono, T. Kataoka, A. Tamura, *J. Biol. Chem.* **2011**, *286*, 39644–39653.
- [15] M. Spoerner, A. Nuehs, P. Ganser, C. Herrmann, A. Wittinghofer, H. R. Kalbitzer, *Biochemistry* **2005**, *44*, 2225–2236.
- [16] I. C. Rosnizeck, T. Graf, M. Spoerner, J. Tränkle, D. Filchtinski, C. Herrmann, L. Gremer, I. R. Vetter, A. Wittinghofer, B. König, H. R. Kalbitzer, *Angew. Chem.* **2010**, *122*, 3918–3922; *Angew. Chem. Int. Ed.* **2010**, *49*, 3830–3833.
- [17] M. Spoerner, T. Graf, B. König, H. R. Kalbitzer, *Biochem. Biophys. Res. Commun.* **2005**, *334*, 709–713.
- [18] I. C. Rosnizeck, M. Spoerner, T. Harsch, S. Kreitner, D. Filchtinski, C. Herrmann, D. Engel, B. König, H. R. Kalbitzer, *Angew. Chem.* **2012**, *124*, 10799–10804; *Angew. Chem. Int. Ed.* **2012**, *51*, 10647–10651.
- [19] F. Shima, Y. Ijiri, S. Muraoka, J. Liao, M. Ye, M. Araki, K. Matsumoto, N. Yamamoto, T. Sugimoto, Y. Yoshikawa, T. Kumasaka, M. Yamamoto, A. Tamura, T. Kataoka, *J. Biol. Chem.* **2010**, *285*, 22696–22705.
- [20] M. T. Mazhab-Jafari, C. B. Marshall, M. Smith, G. M. C. Gasmi-Seabrook, V. Stambolic, R. Rottapel, B. G. Neel, M. Ikura, *J. Biol. Chem.* **2010**, *285*, 5132–5136.
- [21] J. P. Loria, M. Rance, A. G. Palmer, *J. Am. Chem. Soc.* **1999**, *121*, 2331–2332.
- [22] A. Mittermaier, L. E. Kay, *Science* **2006**, *312*, 224–228.
- [23] C. O'Connor, E. L. Kovrigin, *Biochemistry* **2008**, *47*, 10244–10246.
- [24] P. Vallurupalli, G. Bouvignies, L. E. Kay, *J. Am. Chem. Soc.* **2012**, *134*, 8148–8161.
- [25] N. L. Fawzi, J. Ying, R. Ghirlando, D. a Torchia, G. M. Clore, *Nature* **2011**, *480*, 268–272.
- [26] M. J. Smith, B. G. Neel, M. Ikura, *Proc. Natl. Acad. Sci. USA* **2013**, *110*, 4574–4579.
- [27] M. T. Mazhab-Jafari, C. B. Marshall, P. B. Stathopoulos, Y. Kobashigawa, V. Stambolic, L. E. Kay, F. Inagaki, M. Ikura, *J. Am. Chem. Soc.* **2013**, *135*, 3367–3370.
- [28] C. B. Marshall, J. Ho, C. Buerger, M. J. Plevin, G.-Y. Li, Z. Li, M. Ikura, V. Stambolic, *Sci. Signaling* **2009**, *2*, ra3.
- [29] W. H. Press, S. A. Teukolsky, W. T. Vetterling, B. P. Flannery, *Numerical Recipes. The Art of Scientific Computing*, 3rd ed., Cambridge University Press, Cambridge, **2007**.
- [30] Y. Yu, S. Li, X. Xu, Y. Li, K. Guan, E. Arnold, J. Ding, *J. Biol. Chem.* **2005**, *280*, 17093–17100.
-